Original Article

Epicardial fat volume assessment and strain analysis by cardiac magnetic resonance: a novel method for evaluating microcirculation dysfunction after myocardial infarction

Kai Wang[1,2#], Yueyan Wang[1,2#], Yihui Zhao[1,2], Aiqi Chen[1], Xiao Zhang[1,2], Zengwei Cheng[2,3], Mengxiao Liu[4], Yichuan Ma[1]

[1]Department of Radiology, The First Affiliated Hospital of Bengbu Medical University, Bengbu, China; [2]Graduate School of Bengbu Medical University, Bengbu, China; [3]Department of Cardiology, The First Affiliated Hospital of Bengbu Medical University, Bengbu, China; [4]Research Collaboration Team, Diagnostic Imaging, Siemens Healthineers Ltd., Shanghai, China

Contributions: (I) Conception and design: K Wang; (II) Administrative support: None; (III) Provision of study materials or patients: Y Wang; (IV) Collection and assembly of data: Y Zhao; (V) Data analysis and interpretation: All authors; (VI) Manuscript writing: All authors; (VII) Final approval of manuscript: All authors.

[#]These authors contributed equally to this work as co-first authors.

Correspondence to: Yichuan Ma, MM. Professor, Department of Radiology, The First Affiliated Hospital of Bengbu Medical University, No. 110 Hangyuan Road, Alcadía Blue Sky City, Bengbu 233000, China. Email: mayichuan51391@163.com.

Background: In the context of acute ST-segment elevation myocardial infarction (STEMI), epicardial fat volume (EFV) has a significant impact on the formation of microvascular obstruction (MVO). This study aimed to quantitatively measure the EFV and myocardial strain parameters by cardiac magnetic resonance (CMR) and to explore their relationship with the presence or absence of mcrocirculation dysfunction after myocardial infarction.

Methods: This was a retrospective study. From June 2022 to December 2023, 56 consecutive patients diagnosed with acute STEMI who underwent percutaneous coronary intervention (PCI) were selected from The First Affiliated Hospital of Bengbu Medical University. Patients were divided into two groups based on the presence of MVO group and the non-MVO (NMVO) group, with 22 cases (39%) and 34 cases (61%) respectively. The characteristics of the infarction were assessed by delayed enhancement with gadolinium. Based on standard cine images, the global circumferential strain (GCS), global radial strain (GRS), and global longitudinal strain (GLS) of the left and right ventricles were evaluated using CMR feature tracking (CMR-FT) imaging. The volume of EFV was quantified along the short-axis slices of the left and right ventricles at the end of diastole by CMR imaging. The differences in baseline characteristics, EFV, and myocardial strain parameters between the groups were compared using Pearson or Spearman correlation analysis. The specificity and sensitivity of myocardial strain parameters in predicting MVO were obtained using receiver operating characteristic (ROC) curves. The predictive factors for MVO were analyzed using univariate and multivariate logistic regression analyses.

Results: A total of 56 patients were selected, with an average age of 59.84±12.37 years, including 42 males (75%) and 14 females (25%). There was a statistically significant difference in EFV between the MVO group and the NMVO group (P<0.001). The prediction model for MVO based on EFV [area under the ROC curve (AUC): 0.856; 95% confidence interval (CI): 0.736–0.935; sensitivity: 77.27%; specificity: 91.18%], GLS (AUC: 0.929; 95% CI: 0.828–0.980; sensitivity: 90.90%; specificity: 94.12%), GCS (AUC: 0.770; 95% CI: 0.638–0.872; sensitivity: 86.36%; specificity: 61.76%), GRS (AUC: 0.789; 95% CI: 0.659–0.886; sensitivity: 90.19%; specificity: 70.59%). The left ventricular ejection fraction in the MVO group was lower than that in the NMVO group (P=0.001). The GLS, GRS, and GCS in the MVO group were significantly lower than those in the NMVO group (P<0.001). Correlation analysis found that EFV (r=0.602, P<0.001), GLS (r=0.726, P<0.001), GCS (r=0.457, P<0.001) was significantly positively correlated with postoperative myocardial infarction with mcrocirculation obstruction, while GRS (r=–0.486, P<0.001) were negatively correlated with

postoperative myocardial infarction with mcrocirculation obstruction.

Conclusions: After myocardial infarction, there is more EFV in the presence of mcrocirculation dysfunction, and the local myocardial function is reduced more. Monitoring EFV plays a significant role in the early anti-lipid treatment strategy for patients with MVO.

Keywords: Cardiac magnetic resonance feature tracking technology (CMR-FT technology); epicardial fat volume (EFV); acute myocardial infarction (AMI); microvascular obstruction (MVO)

Submitted Jul 27, 2024. Accepted for publication Dec 06, 2024. Published online Feb 21, 2025.
doi: 10.21037/cdt-24-359
View this article at: https://dx.doi.org/10.21037/cdt-24-359

Introduction

Acute ST-segment elevation myocardial infarction (STEMI) is a severe type of coronary heart disease, primarily due to coronary artery obstruction leading to acute ischemic necrosis of the myocardium. Despite a decline in STEMI with the improvement in medical standards and lifestyle, it remains a significant public health issue worldwide, especially in developing countries. Prevention and early intervention are key to reducing the incidence of STEMI and improving prognosis.

The goal of STEMI treatment is to restore myocardial perfusion as quickly as possible, save the myocardium, and prevent infarct expansion. Current reperfusion therapies mainly involve percutaneous coronary intervention (PCI) or thrombolysis. However, after the culprit vessel is reopened, microcirculation reperfusion cannot be fully guaranteed, leading to areas of no reflow in the myocardial ischemic region, known as microvascular obstruction (MVO). MVO can be seen in patients with acute myocardial infarction (AMI) after coronary artery occlusion reperfusion (1), some patients with acute extensive myocardial ischemia, and those with late MVO (2). Its characteristic is the damage and dysfunction of the myocardial microvascular system, with no reflow phenomenon in the infarct area (3), ultimately leading to reduced tissue perfusion and the formation of an infarct zone, mainly extending from the endocardium to the epicardium (4,5). Cardiac magnetic resonance (CMR) imaging is the gold standard for MVO assessment, with MVO appearing as low signal areas within the late gadolinium enhanced (LGE) myocardial region (6). Cardiac imaging plays a crucial role in the diagnosis and treatment process of MVO. Contrast-enhanced steady-state free precession (CE-SSFP) technology combines LGE and steady-state free precession, accurately quantifying MVO, while CMR imaging has a unique ability to extensively analyze cardiac deformation, volume, myocardial morphology, and tissue composition, with increasing evidence of its importance for prognosis and superiority over currently used clinical parameters (7).

Epicardial adipose tissue (EAT) serves as a fat storage reservoir in the heart and plays an important role in cardiac lipid metabolism, deposited between the myocardium and the visceral layer of the pericardium, covering more than 60% of the heart surface and accounting for about 20% of heart weight (8). Studies have found that EAT has potential roles in the progression of ventricular structural changes, functional pathophysiological changes, and clinical evolution in the context of AMI (9-11). Ultrasound is the

Highlight box

Key findings

- This study constructs a combined model of epicardial fat volume (EFV) and myocardial strain to enhance the diagnostic performance for microvascular obstruction (MVO).

What is known and what is new?

- Previous research shown that the volume of epicardial adipose tissue is associated with an increased incidence of cardiovascular disease.
- Previous studies have shown that myocardial strain has a high diagnostic efficiency for early changes in the heart.
- This study constructs a combined model of EFV and myocardial strain to enhance the diagnostic performance for MVO.

What is the implication, and what should change now?

- The monitoring of EFV plays a crucial role in the clinical assessment, treatment decision-making, and prognosis evaluation for patients with myocardial infarction complicated by microcirculatory dysfunction. It provides a valuable biomarker for clinical practice and guides the selection of early anti-lipid treatment strategies.

simplest, convenient, and highly safe method for measuring EAT, directly detecting the thickness of EAT at the right ventricular free wall to assess the overall distribution of EAT in the heart. Although this method is non-invasive, fast, and relatively inexpensive, it has many obvious limitations. Ultrasound finds it difficult to differentiate EAT or pericardial fat and may be affected by the operator's technique and many other factors. Compared to ultrasound, spiral computed tomography (CT) not only accurately measures the thickness of EAT at each level but also has the advantage of repeatable operation. After certain post-processing on the computer, the overall epicardial fat volume (EFV) can be obtained. However, coronary CT angiography (CTA) examination must be completed with intravenous injection of iodinated contrast agents and emits certain radiation to the human body.

Magnetic resonance imaging (MRI) is a non-invasive, non-ionizing radiation, high soft tissue resolution technique, with significant advantages in the quantitative measurement of fat in some visceral organs. At the same time, CMR can meticulously depict cardiac structure and function and provide more accurate and quantitative assessments of ventricular volume, myocardial mass, and cardiac function. Myocardial strain measures the spatial vectors in the longitudinal, axial, and radial predefined directions during the entire cardiac cycle using an internal coordinate system aligned with the three axes of the heart. Longitudinal strain (LS) refers to longitudinal shortening, radial strain (RS) refers to radial thickening, and circumferential strain (CS) refers to circumferential rotation (12). Myocardial strain can be divided into global myocardial strain and segmental myocardial strain, usually referring to the 17-segment division of the left ventricle by the American Heart Association. Previous studies have shown that myocardial strain has a high diagnostic efficiency for early changes in the heart. After AMI, myocardial contractile function is impaired, and animal experiments and clinical studies have confirmed significant changes in myocardial strain after AMI. Animal experiments have found that global CS (GCS) is significantly reduced on both early 9±2 days and late 33±10 days after myocardial infarction compared to before infarction, and studies have shown that the myocardial strain in the remote area of myocardial infarction decreases after the occurrence of heart failure compared to before the occurrence of heart failure, with global LS (GLS) being a more sensitive parameter for assessing local myocardial dysfunction (13).

As a parameter that has emerged in recent years to evaluate the overall and local movement and function of the myocardium, myocardial strain is increasingly widely used in non-invasive assessment of the heart. CMR, with its high resolution and one-stop non-invasive assessment of the heart, is currently recognized as the gold standard for quantitative evaluation of changes in cardiac tissue function after myocardial infarction (14).

Therefore, this study uses CMR to explore the degree of impairment of myocardial strain in myocardial infarction of different degrees and its impact on local left ventricular function, and to quantitatively analyze EFV, discuss the relationship with MVO, and provide a basis for early clinical evaluation and treatment. We present this article in accordance with the STARD reporting checklist (available at https://cdt.amegroups.com/article/view/10.21037/cdt-24-359/rc).

Methods

General data and grouping

STEMI patients who were admitted to The First Affiliated Hospital of Bengbu Medical University from June 2022 to December 2023 were included in this retrospective study. Inclusion criteria: (I) diagnosed with STEMI according to the diagnostic criteria of the European Society of Cardiology (15); (II) first-time myocardial infarction, successfully treated with PCI; and (III) first CMR examination with image quality meeting the requirements. Exclusion criteria: (I) history of myocardial infarction; (II) history of PCI or coronary artery bypass grafting; and (III) contraindications for LGE-CMR examination (such as claustrophobia, etc.). After exclusion, a total of 80 STEMI patients were enrolled. Finally, 56 STEMI patients were included. The flow diagram refers to *Figure 1*. All patients underwent CMR examination within 6.1±2.2 days after PCI. The absence of low signal areas in the magnetic resonance (MR) delayed enhancement high signal infarcted myocardium was defined as the non-MVO (NMVO) group, and the presence of low signal areas in the MR delayed enhancement high signal infarcted myocardium was defined as the MVO group. The study was conducted in accordance with the Declaration of Helsinki (as revised in 2013). The study received approval from the Ethics Committee of The First Affiliated Hospital of Bengbu Medical University (No. 2023YJS287). Patient informed consent was exempted given the retrospective nature of the study.

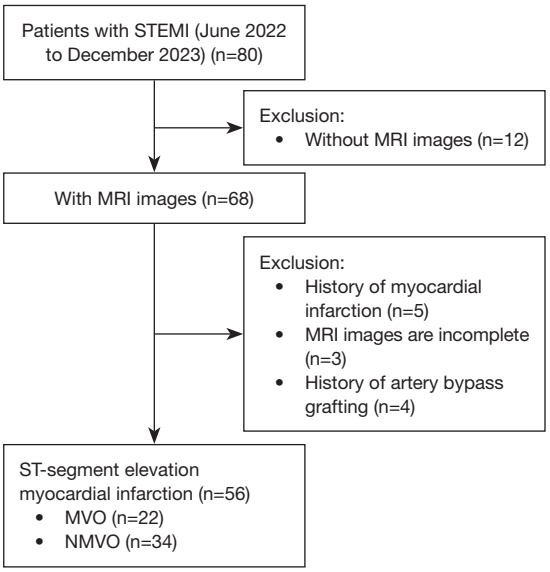

Figure 1 Flow diagram of patient selection. STEMI, ST-segment elevation myocardial infarction; MRI, magnetic resonance imaging; MVO, microvascular obstruction; NMVO, non-microvascular obstruction.

Research methods

CMR examination

All patients using the Siemens MAGNETOM Avanto 1.5-T magnetic resonance scanner (Siemens, Earlangen, Germany) equipped in the Radiology Department of The First Affiliated Hospital of Bengbu Medical University. The main scanning sequences included: ventricular short-axis, two-chamber, three-chamber, and four-chamber heart views with balanced steady-state free precession (bSSFP) cine imaging, triple inversion recovery (IR) sequence ventricular short-axis, and LGE. The parameters for the cine sequence were set as follows: repetition time (TR) 2.84 ms, echo time (TE) 1.25 ms, flip angle 180°, slice thickness 6.0 mm, resolution 1.4 mm × 1.8 mm. The LGE used an electrocardiogram (ECG)-triggered inversion recovery fast gradient echo sequence, with gadolinium-diethylene triamine pentaacetate (Gd-DTPA) contrast agent injected intravenously at a dose of 0.15 mmol/kg, starting the scan 10–30 minutes after the delay, with the following parameters: TR 904 ms, TE 1.98 ms, flip angle 20°, slice thickness 6.0 mm, resolution 1.4 mm × 1.9 mm.

Image processing

The images were uploaded to the CVi42 software platform (Circle Cardiovascular Imaging, Calgary, Canada) for post-processing, and all images were independently analyzed by two radiologists with over 5 years of experience in cardiac radiology. The observer performing the strain analysis was blinded to the baseline CMR parameters and advanced tissue characterization. Using the software's built-in analysis functions, the endocardial and epicardial boundaries of the left ventricle at the end of systole and diastole in the two-, three-, and four-chamber heart views of the long-axis, and the basal, papillary muscle, and apical segments of the short-axis were manually outlined using a semi-automatic method. The papillary muscle was included in the ventricular cavity; the CMR software divided the left ventricular endocardium into 48 characteristic points and automatically tracked the endocardial and epicardial boundaries, calculating cardiac function parameters and myocardial strain indicators. The observer analyzed all CMR short-axis images using dedicated post-processing software (CVi42), Cardiac adipose tissue was quantified on all short-axis slices (base to apex) in end-diastolic phase, After the delineation was completed, the software automatically calculated the EFV, as shown in *Figure 2*. MVO, identifiable as a no-reflow area within the myocardial infarction characterized by a hypointense signal in the delayed enhancement images, is depicted in *Figure 3*.

Statistical analysis

We used the Shapiro-Wilk and Kolmogorov-Smirnov tests to examine the normal distribution. Quantitative variables of data conforming to the normal distribution and non-normal distribution were represented by mean ± standard deviation and median [range or interquartile range (IQR)], respectively, while qualitative variable data were represented by n (%). The Mann-Whitney *U* test (Chi-squared test) was used to compare continuous variable datasets and non-parametric data. The two independent sample *t*-tests were used for comparison between the MVO group and the NMVO group. The results of the count data were represented by the number of cases or the percentage of the total, and the group comparison was made using the Chi-squared test. Univariate and multivariate logistic regression analyses were used to determine the independent predictive factors for MVO, with variables with P values <0.10 in the univariate analysis being included in the multivariate model. The predictive value of the EFV indicator for MVO was evaluated using the area under the receiver operating characteristic (ROC) curve (AUC). Cardiac function and myocardial strain parameters were analyzed using Pearson's

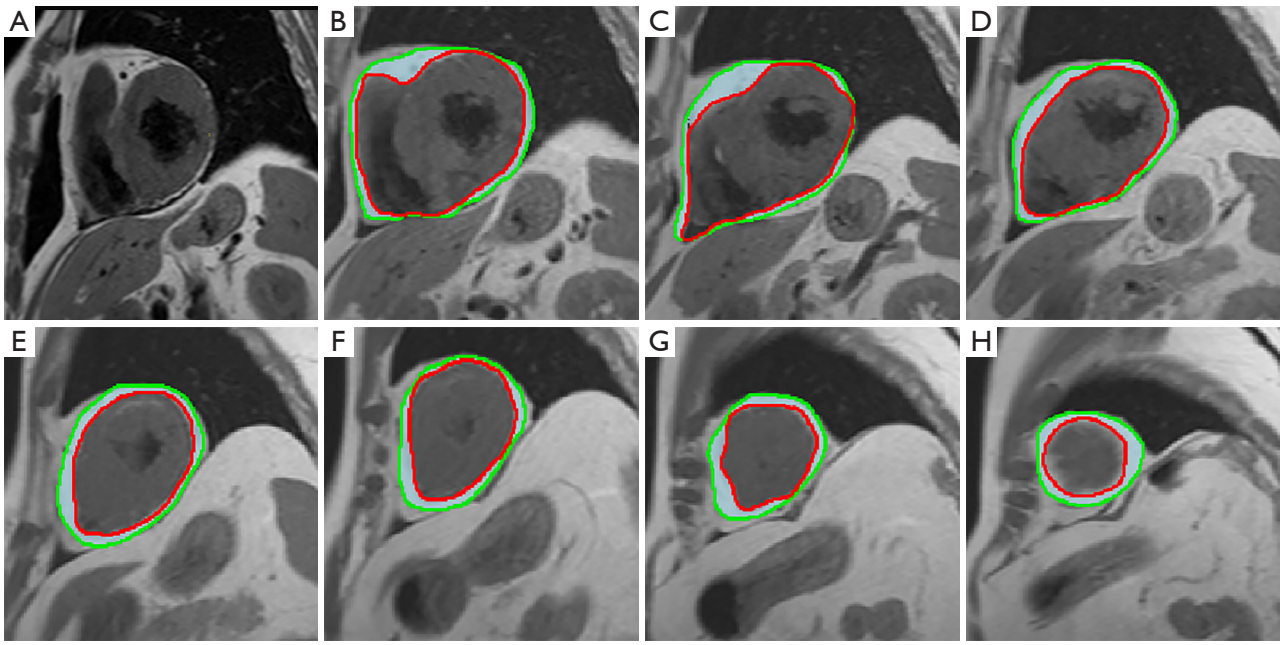

Figure 2 Short-axis MR slices for different levels (basal to apical). (A) Not sketch level, step by step (B-H) sketch different levels of short-axis after MRI slices. Red line: myocardial intima; green line: pericardial; light green line: EAT. MR, magnetic resonance; MRI, magnetic resonance imaging; EAT, epicardial adipose tissue.

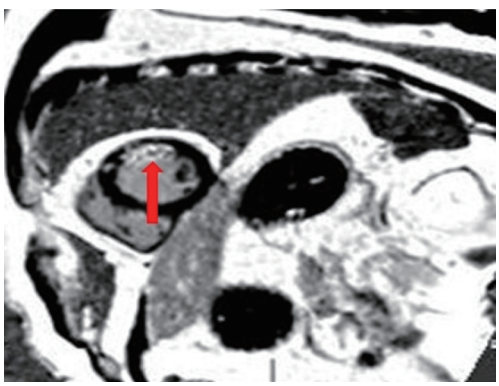

Figure 3 A 58-year-old male with an acute anterior myocardial infarction following PCI shows a hypointense area (red arrow) on delayed enhancement. PCI, percutaneous coronary intervention.

correlation analysis, with correlation coefficients of 0.8–1.0 being extremely strong, 0.6–0.7 being strong, 0.4–0.5 being moderate, 0.2–0.3 being weak, and 0.0–0.1 being extremely weak or no correlation. All analyses were performed using SPSS 26 (IBM, Chicago, IL, USA), Medcalc 20.0 (Medcalc, Ostend, Belgium), and GraphPad Prism (Prism 9 for Windows, San Diego, CA, USA). A two-tailed P value <0.05 was considered statistically significant.

Results

Comparison of clinical data of patients

A retrospective study was conducted on 56 patients who underwent PCI diagnosed with acute STEMI by coronary angiography at The First Affiliated Hospital of Bengbu Medical University from June 2022 to December 2023. There were 42 male patients (accounting for 75%) with an average age of 59.84±12.37 years. There were no significant differences in age, male gender, body surface area (BSA), underlying diseases, left ventricular end-diastolic volume, left ventricular end-systolic volume, and left ventricular end-diastolic diameter between the two groups (P>0.05). However, the left ventricular ejection fraction in the MVO group was significantly lower than that in the NMVO group (P=0.001), and the heart rate in the MVO group was higher than that in the NMVO group. As shown in *Table 1*.

Diagnostic efficacy of EFV, myocardial strain, and combined analysis for MVO

The GLS, global RS (GRS), and GCS in the MVO group were all significantly lower than those in the NMVO group (P<0.001); the EFV in the MVO group was higher than that

Table 1 Clinical data

Variables	MVO (n=22)	NMVO (n=34)	χ^2/t	P
Age (years)	61.86±13.61	58.53±11.51	−0.95	0.35
BSA (m^2)	1.89±1.85	1.78±1.14	−1.63	0.11
Hypertensive	12 (54.5)	15 (44.1)	0.582†	0.45
Diabetes	4 (18.2)	5 (14.7)	0.118†	0.73
Smoking	5 (22.7)	7 (20.6)	0.036†	0.85
Heart rate (n/min)	86.33±18.98	74.22±11.89	−2.94	0.005
LVEF (%)	37.33±14.88	49.82±7.52	3.66	0.001
CO (%)	4.68±1.55	4.47±1.58	−0.49	0.62
Cardiac index (%)	2.50±0.82	2.49±0.76	−0.09	0.93
LVEDV (mL)	170.02±45.56	148.39±51.62	−1.60	0.12
LVESV (mL)	108.65±50.29	87.81±46.76	−1.94	0.053

Data are presented as n (%) or mean ± standard deviation. †, Chi-squared test. MVO, microvascular obstruction; NMVO, non-microvascular obstruction; BSA, body surface area; LVEF, left ventricular ejection fraction; CO, cardiac output; LVEDV, left ventricular end-diastolic volume; LVESV, left ventricular end-systolic volume.

Table 2 Myocardial strain and EFV parameter analysis

Variables	MVO (n=22)	NMVO (n=34)	*t*	P
GRS (%)	14.64±5.87	21.98±6.70	4.20	<0.001
GCS (%)	−10.90±4.89	−16.06±5.36	−3.64	<0.001
GLS (%)	−5.91±2.63	−10.62±3.01	−5.99	<0.001
EFV (cm^3)	83.73±16.52	58.06±15.36	−5.93	<0.001

Data are presented as mean ± standard deviation. Negative values of GCS and GLS indicate that the myocardium has undergone normal physiological shortening during the contraction process, which is a part of the heart's pumping function. EFV, epicardial fat volume; MVO, microvascular obstruction; NMVO, non-microvascular obstruction; GRS, global radial strain; GCS, global circumferential strain; GLS, global longitudinal strain.

in the NMVO group (P<0.001). The ROC curve analysis showed that among the three, the best diagnostic efficacy was for GLS (AUC: 0.929; sensitivity: 90.90%; specificity: 94.12%), with a Youden index of 0.85. EFV predicted MVO (AUC: 0.856; sensitivity: 77.27%; specificity: 91.18%); as shown in *Tables 2,3*.

Correlation between EFV and global myocardial strain parameters of the left ventricle

First, the EFV was normalized using BSA to obtain the normalized EFV (EFVnormalized). A scatter plot of EFVnormalized and global myocardial strain parameters of the left ventricle for 22 patients in the MVO group was drawn, as shown in *Figure 4*. Pearson correlation analysis showed that GRS (r=−0.38, P=0.08) and GLS (r=0.26, P=0.63) had a weak correlation with EFV, while the correlation between GCS (r=0.11, P=0.24) with EFV was weaker and not statistically significant.

ROC curves for predicting MVO using EFV, myocardial strain, and combined diagnosis

The ROC of the combined analysis predicted MVO [AUC: 0.945; 95% confidence interval (CI): 0.850–0.988; sensitivity 95.45%; specificity 91.59%]; the AUC value and sensitivity were higher than those of single diagnosis, as shown in *Figure 5*.

Table 3 Diagnostic efficacy of EFV, myocardial strain, and combined analysis for MVO

Variables	AUC	Sensitivity (%)	Specificity (%)	95% CI	P	Youden index
GRS (%)	0.789	90.19	70.59	0.659–0.886	<0.001	0.6150
GCS (%)	0.770	86.36	61.76	0.638–0.872	<0.001	0.485
GLS (%)	0.929	90.90	94.12	0.828–0.980	<0.001	0.850
EFV (cm^3)	0.856	77.27	91.18	0.736–0.935	<0.001	0.685
Unite	0.945	95.45	91.59	0.850–0.988	<0.001	0.886

Unite: combined model based on GCS, GLS, GRS, and EFV. EFV, epicardial fat volume; MVO, microvascular obstruction; AUC, area under the ROC curve; ROC, receiver operating characteristic; CI, confidence interval; GRS, global radial strain; GCS, global circumferential strain; GLS, global longitudinal strain.

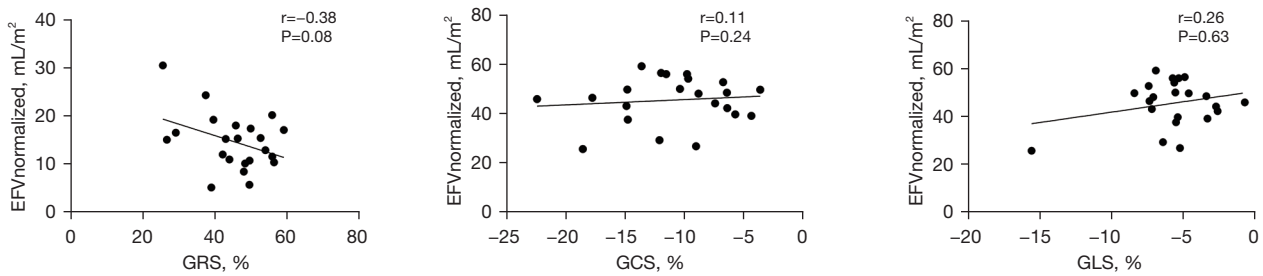

Figure 4 GRS, GCS, GLS, and EFV linear relationship. EFVnormalized, the EFV was normalized using BSA to obtain the normalized EFV. EFV, epicardial fat volume; BSA, body surface area; GRS, global radial strain; GCS, global circumferential strain; GLS, global longitudinal strain.

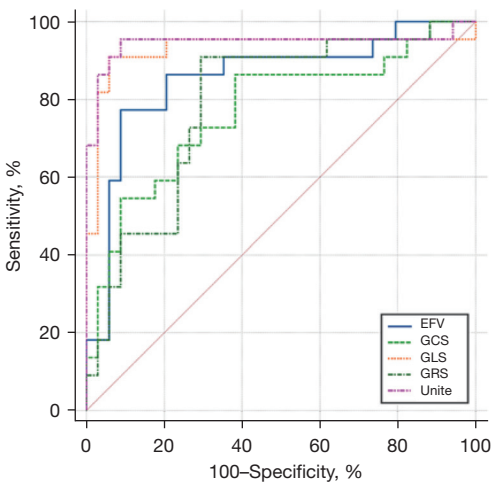

Figure 5 ROC curve of combined analysis of CMR parameters and EFV in the diagnosis of microcirculatory disturbance in STEMI patients after PCI. EFV, epicardial fat volume; GCS, global circumferential strain; GLS, global longitudinal strain; GRS, global radial strain; ROC, receiver operating characteristic; CMR, cardiac magnetic resonance; STEMI, ST-segment elevation myocardial infarction; PCI, percutaneous coronary intervention.

Independent predictive parameters for MVO based on multivariate logistic regression analysis

In multivariate logistic regression, GLS [odds ratio (OR) =1.910; 95% CI: 1.137–3.206; P=0.01] and EFV (OR =1.077; 95% CI: 1.013–1.144; P=0.02) were independent predictive factors for MVO, as shown in *Table 4* and *Figure 6*.

Correlation between MVO and EFV, left ventricular global myocardial strain parameters

Spearman correlation analysis showed that EFV (r=0.602, P<0.001), GLS (r=0.726, P<0.001), GCS (r=0.457, P<0.001) was significantly positively correlated with postoperative myocardial infarction with mcrocirculation obstruction, while GRS (r=−0.486, P<0.001) were negatively correlated with postoperative myocardial infarction with mcrocirculation obstruction, as shown in *Table 5*.

Discussion

Studies have shown that the volume of EAT is associated

Table 4 Univariable and multivariable predictors of presence of MVO

Variables	Univariable analysis		Multivariable analysis	
	OR (95% CI)	P	OR (95% CI)	P
GRS (%)	0.834 (0.739–0.919)	<0.001	1.076 (0.894–1.295)	0.44
GCS (%)	1.250 (0.097–1.472)	0.003	1.113 (0.904–1.370)	0.31
GLS (%)	2.161 (1.550–3.536)	<0.001	1.910 (1.137–3.206)	0.01
EFV (%)	1.095 (1.052–1.153)	<0.001	1.077 (1.013–1.144)	0.02
LVEF (%)	0.897 (0.829–0.953)	0.002	0.886 (0.757–1.044)	0.12
HR (n/min)	1.012 (1.005–1.088)	0.04	0.959 (0.879–1.046)	0.34

MVO, microvascular obstruction; OR, odds ratio; CI, confidence interval; GRS, global radial strain; GCS, global circumferential strain; GLS, global longitudinal strain; EFV, epicardial fat volume; LVEF, left ventricular ejection fraction; HR, heart rate.

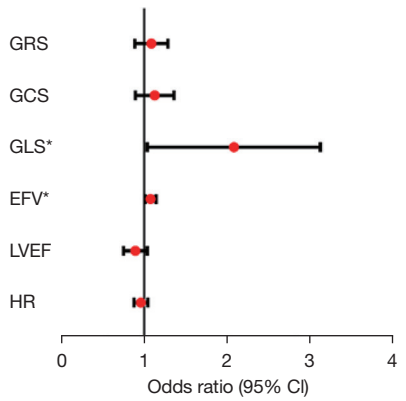

Figure 6 Multivariate logistic regression analysis to identify the risk factors associated with the occurrence of MVO in patients with STEMI. *, GLS and EFV were independent predictive factors for MVO. GRS, global radial strain; GCS, global circumferential strain; GLS, global longitudinal strain; EFV, epicardial fat volume; LVEF, left ventricular ejection fraction; HR, heart rate; CI, confidence interval; MVO, microvascular obstruction; STEMI, ST-segment elevation myocardial infarction.

Table 5 Correlation between MVO and EFV, left ventricular global myocardial strain

Variables	MVO	
	r	P
GLS (%)	0.726	<0.001
GRS (%)	–0.486	<0.001
GCS (%)	0.457	<0.001
EFV (cm^3)	0.602	<0.001

MVO, microvascular obstruction; EFV, epicardial fat volume; GLS, global longitudinal strain; GRS, global radial strain; GCS, global circumferential strain.

with an increased incidence of cardiovascular disease (CVD) (16). However, there is limited research on its impact on MVO after myocardial infarction. Additionally, they all analyze the relationship between MVO and EFV with myocardial strain separately. Therefore, this study constructs a combined model of EFV and myocardial strain to enhance the diagnostic performance for MVO. Meanwhile, this study primarily explored the correlation between EFV and MVO and left ventricular myocardial strain in patients after AMI who underwent PCI. In the study, we used CMR and tissue tracking technology to quantify left ventricular myocardial function. When measuring EFV, CMR was used for quantitative measurement of EFV, rather than cardiac CT volume measurement or echocardiographic local thickness measurement. The final analysis results showed that after myocardial infarction, the MVO group had more EFV content and greater reduction in GLS, GRS, and GCS compared to the NMVO group. Multivariate regression analysis indicated that GLS and EFV are independent influencing factors for MVO after myocardial infarction.

EAT is deposited in the fat layer between the pericardium and myocardium, closely contacting the myocardium, and there is no fascial tissue between them (17). It has a mechanical protective effect on the heart and can directly transport fatty acids to the myocardium, serving as an energy source for the myocardium (18). EAT also participates in the synthesis, production, and secretion of various bioactive molecules (19,20), and is the main source of a large number of free fatty acids and bioactive molecules (such as adiponectin, leptin, and inflammatory cytokines). However, excessive secretion of fatty acids by EAT exceeds the myocardial oxidation capacity, leading

to the accumulation of intermediates such as ceramides, which in turn leads to myocardial cell apoptosis and fibrosis (21,22). An increase in EFV increases the secretion of pro-inflammatory adipokines (leptin, mucin, interleukin-1β, interleukin-6, and antibodies), directly causing an increase in paracrine effects leading to inflammation and fibrosis in adjacent myocardium (23,24). Additionally, the protective or harmful effects of EAT on coronary arteries and myocardial cells mainly depend on the relationship between EAT and the microenvironment (20,25). In patients who undergo PCI after AMI, factors such as cytotoxic factors, inflammatory reactions, and vasoconstriction, as well as microthrombi caused by atherosclerotic debris in the distal lumen, platelet plugging, and cellular edema after reperfusion, can lead to MVO (26,27). After the acute phase, MVO gradually fibroses during the formation of myocardial scar tissue. Therefore, an increase in EFV in such patients indicates the occurrence of MVO, suggesting a more severe degree of myocardial infarction (28,29). In this study, the MVO group had more EFV content than the NMVO group. Based on the EFV content, a prediction model for myocardial infarction with combined MVO was constructed, with an AUC value of 0.856, a sensitivity of 77.27%, and a specificity of 91.18%.

Due to the highly complex functional changes in acute STEMI, it is particularly important to comprehensively assess left ventricular function in the early stages after STEMI (30). CMR strain technology can well diagnose and assess the early stages of ischemic myocardial dysfunction that are not easily detected by conventional diagnostic methods (31). This study showed that the LVEF, GLS, GRS, and GCS in the MVO group were lower than those in the NMVO group. GLS has a significantly higher diagnostic efficacy for MVO after PCI in STEMI patients than GCS and GRS, which is consistent with previous studies (32). In the studies by Cherian *et al.* and Zhang *et al.*, GLS was proven to be a strong predictor of left ventricular remodeling and adverse events (such as congestive heart failure and death) (23,33). This may be because the irreversible myocardial ischemia caused by STEMI first affects the longitudinal myocardial fibers of the subendocardium, thereby affecting the longitudinal myocardial contraction represented by GLS (33).

In this study, correlation analysis showed that EFV, GLS, and GCS were significantly positively correlated with postoperative myocardial infarction combined with MVO; while GRS, were negatively correlated with postoperative myocardial infarction combined with MVO. The diagnostic sensitivity and AUC value of myocardial strain parameters (GLS, GRS, GCS) combined with EFV volume in MVO after PCI in STEMI patients were higher than those of single diagnosis. In the analysis of the correlation between EFV and global myocardial strain parameters of the left ventricle, it was found that GRS and GLS had a weak correlation with EFV, and an extremely weak correlation with GCS. This indicates that the changes in cardiac function after myocardial infarction cannot be predicted by a single condition alone; it is necessary to combine clinical symptoms, routine blood indicators such as N-terminal pro-brain natriuretic peptide (NT-proBNP), and other indicators for joint analysis. CMR, as a non-invasive, radiation-free imaging method, can provide various quantitative indicators (myocardial strain capacity, infarct area size, microcirculation resistance index, etc.), all of which are important parameters for evaluating the patient's cardiac function status (34-36).

Limitations

Due to the small sample size of this experiment and only studying the overall strain parameters, and the lack of detailed classification and treatment of the infarct area combined with intramyocardial hemorrhage (IMH), further research and expansion of the sample size are still needed. Secondly, this study found that EFV is an independent determinant of MVO, indicating that to some extent, an increase in EFV content is a partial cause of the occurrence of MVO and left ventricular myocardial dysfunction and reduced myocardial strain, but the specific mechanism still needs further research.

Conclusions

In summary, through CMR imaging, a close correlation between EFV and MVO can be found, which can serve as an important functional imaging parameter for acute myocardial pathological changes in patients with acute STEMI. Combined with GLS, GRS, GCS, and clinical-related indicators, it can provide prognosis assessment and treatment strategies for clinical practice.

Acknowledgments

None.

Footnote

Reporting Checklist: The authors have completed the STARD reporting checklist. Available at https://cdt.amegroups.com/article/view/10.21037/cdt-24-359/rc

Data Sharing Statement: Available at https://cdt.amegroups.com/article/view/10.21037/cdt-24-359/dss

Peer Review File: Available at https://cdt.amegroups.com/article/view/10.21037/cdt-24-359/prf

Funding: None.

Conflicts of Interest: All authors have completed the ICMJE uniform disclosure form (available at https://cdt.amegroups.com/article/view/10.21037/cdt-24-359/coif). M.L. is a current employee of Siemens Healthineers Ltd., Shanghai. The other authors have no conflicts of interest to declare.

Ethical Statement: The authors are accountable for all aspects of the work in ensuring that questions related to the accuracy or integrity of any part of the work are appropriately investigated and resolved. The study was conducted in accordance with the Declaration of Helsinki (as revised in 2013). The study received approval from the Ethics Committee of The First Affiliated Hospital of Bengbu Medical University (No. 2023YJS287). Patient informed consent was exempted given the retrospective nature of the study.

References

1. Ghobrial M, Bawamia B, Cartlidge T, et al. Microvascular Obstruction in Acute Myocardial Infarction, a Potential Therapeutic Target. J Clin Med 2023;12:5934.
2. Doenst T, Haverich A, Serruys P, et al. PCI and CABG for Treating Stable Coronary Artery Disease: JACC Review Topic of the Week. J Am Coll Cardiol 2019;73:964-76.
3. Abbas A, Matthews GH, Brown IW, et al. Cardiac MR assessment of microvascular obstruction. Br J Radiol 2015;88:20140470.
4. Niccoli G, Burzotta F, Galiuto L, et al. Myocardial no-reflow in humans. J Am Coll Cardiol 2009;54:281-92.
5. Niccoli G, Scalone G, Lerman A, et al. Coronary microvascular obstruction in acute myocardial infarction. Eur Heart J 2016;37:1024-33.
6. Mather AN, Lockie T, Nagel E, et al. Appearance of microvascular obstruction on high resolution first-pass perfusion, early and late gadolinium enhancement CMR in patients with acute myocardial infarction. J Cardiovasc Magn Reson 2009;11:33.
7. Abbasi SA, Ertel A, Shah RV, et al. Impact of cardiovascular magnetic resonance on management and clinical decision-making in heart failure patients. J Cardiovasc Magn Reson 2013;15:89.
8. Villasante Fricke AC, Iacobellis G. Epicardial Adipose Tissue: Clinical Biomarker of Cardio-Metabolic Risk. Int J Mol Sci 2019;20:5989.
9. Islas F, Gutiérrez E, Cachofeiro V, et al. Importance of cardiac imaging assessment of epicardial adipose tissue after a first episode of myocardial infarction. Front Cardiovasc Med 2022;9:995367.
10. Napoli G, Pergola V, Basile P, et al. Epicardial and Pericoronary Adipose Tissue, Coronary Inflammation, and Acute Coronary Syndromes. J Clin Med 2023;12:7212.
11. Ren Y, Chen L, Liu J, et al. Correlation of epicardial adipose tissue and inflammatory indices in patients with STEMI and implications for atrial arrhythmias. Int J Cardiol 2024;406:132016.
12. Korosoglou G, Giusca S, Hofmann NP, et al. Strain-encoded magnetic resonance: a method for the assessment of myocardial deformation. ESC Heart Fail 2019;6:584-602.
13. Espe EKS, Aronsen JM, Eriksen M, et al. Regional Dysfunction After Myocardial Infarction in Rats. Circ Cardiovasc Imaging 2017;10:e005997.
14. Ibanez B, Aletras AH, Arai AE, et al. Cardiac MRI Endpoints in Myocardial Infarction Experimental and Clinical Trials: JACC Scientific Expert Panel. J Am Coll Cardiol 2019;74:238-56.
15. Ibanez B, James S, Agewall S, et al. 2017 ESC Guidelines for the management of acute myocardial infarction in patients presenting with ST-segment elevation: The Task Force for the management of acute myocardial infarction in patients presenting with ST-segment elevation of the European Society of Cardiology (ESC). Eur Heart J

2018;39:119-77.
16. Wang Z, Song T, Yu D, et al. Correlation analysis of epicardial adipose tissue and ventricular myocardial strain in Chinese amateur marathoners using cardiac magnetic resonance. PLoS One 2022;17:e0274533.
17. Al-Talabany S, Mordi I, Graeme Houston J, et al. Epicardial adipose tissue is related to arterial stiffness and inflammation in patients with cardiovascular disease and type 2 diabetes. BMC Cardiovasc Disord 2018;18:31.
18. Iacobellis G. Epicardial adipose tissue in contemporary cardiology. Nat Rev Cardiol 2022;19:593-606.
19. Iacobellis G, Bianco AC. Epicardial adipose tissue: emerging physiological, pathophysiological and clinical features. Trends Endocrinol Metab 2011;22:450-7.
20. Iacobellis G, Corradi D, Sharma AM. Epicardial adipose tissue: anatomic, biomolecular and clinical relationships with the heart. Nat Clin Pract Cardiovasc Med 2005;2:536-43.
21. Antonopoulos AS, Papastamos C, Cokkinos DV, et al. Epicardial Adipose Tissue in Myocardial Disease: From Physiology to Heart Failure Phenotypes. Curr Probl Cardiol 2023;48:101841.
22. Diab A, Dastmalchi LN, Gulati M, et al. A Heart-Healthy Diet for Cardiovascular Disease Prevention: Where Are We Now? Vasc Health Risk Manag 2023;19:237-53.
23. Cherian S, Lopaschuk GD, Carvalho E. Cellular cross-talk between epicardial adipose tissue and myocardium in relation to the pathogenesis of cardiovascular disease. Am J Physiol Endocrinol Metab 2012;303:E937-49.
24. Packer M. Epicardial Adipose Tissue May Mediate Deleterious Effects of Obesity and Inflammation on the Myocardium. J Am Coll Cardiol 2018;71:2360-72.
25. Mazurek T, Zhang L, Zalewski A, et al. Human epicardial adipose tissue is a source of inflammatory mediators. Circulation 2003;108:2460-6.
26. Zhao J, Cheng W, Dai Y, et al. Excessive accumulation of epicardial adipose tissue promotes microvascular obstruction formation after myocardial ischemia/reperfusion through modulating macrophages polarization. Cardiovasc Diabetol 2024;23:236.
27. Reffelmann T, Kloner RA. The no-reflow phenomenon: A basic mechanism of myocardial ischemia and reperfusion. Basic Res Cardiol 2006;101:359-72.
28. Silva M, Paiva L, Teixeira R, et al. Microcirculation function assessment in acute myocardial infarction: A systematic review of microcirculatory resistance indices. Front Cardiovasc Med 2022;9:1041444.
29. Hausenloy DJ, Yellon DM. Myocardial ischemia-reperfusion injury: a neglected therapeutic target. J Clin Invest 2013;123:92-100.
30. Bodi V. Strain by Feature Tracking: A Short Summary of the Journey of CMR in STEMI. JACC Cardiovasc Imaging 2019;12:1199-201.
31. Nunes MCP, Badano LP, Marin-Neto JA, et al. Multimodality imaging evaluation of Chagas disease: an expert consensus of Brazilian Cardiovascular Imaging Department (DIC) and the European Association of Cardiovascular Imaging (EACVI). Eur Heart J Cardiovasc Imaging 2018;19:459-460n.
32. Kidambi A, Mather AN, Motwani M, et al. The effect of microvascular obstruction and intramyocardial hemorrhage on contractile recovery in reperfused myocardial infarction: insights from cardiovascular magnetic resonance. J Cardiovasc Magn Reson 2013;15:58.
33. Zhang M, Lu Y, Li Z, et al. Value of Fast MVO Identification From Contrast-Enhanced Cine (CE-SSFP) Combined With Myocardial Strain in Predicting Adverse Events in Patients After ST-Elevation Myocardial Infarction. Front Cardiovasc Med 2022;8:804020.
34. Dastidar AG, Harries I, Pontecorboli G, et al. Native T1 mapping to detect extent of acute and chronic myocardial infarction: comparison with late gadolinium enhancement technique. Int J Cardiovasc Imaging 2019;35:517-27.
35. Reindl M, Holzknecht M, Tiller C, et al. Impact of infarct location and size on clinical outcome after ST-elevation myocardial infarction treated by primary percutaneous coronary intervention. Int J Cardiol 2020;301:14-20.
36. Doherty DJ, Sykes R, Mangion K, et al. Predictors of Microvascular Reperfusion After Myocardial Infarction. Curr Cardiol Rep 2021;23:21.

Cite this article as: Wang K, Wang Y, Zhao Y, Chen A, Zhang X, Cheng Z, Liu M, Ma Y. Epicardial fat volume assessment and strain analysis by cardiac magnetic resonance: a novel method for evaluating microcirculation dysfunction after myocardial infarction. Cardiovasc Diagn Ther 2025;15(1):137-147. doi: 10.21037/cdt-24-359

